Eur. Phys. J. D **20**, 37–44 (2002)
DOI: 10.1140/epjd/e2002-00116-1

THE EUROPEAN PHYSICAL JOURNAL D

Level lifetimes in 3p and 3d configurations of Fe XII

E. Biémont[1,2], P. Palmeri[2], P. Quinet[1,2], E. Träbert[1,3,a], and C.J. Zeippen[4]

[1] Institut de Physique Nucléaire, Atomique et de Spectroscopie (IPNAS), Université de Liège, Sart Tilman Bâtiment 15, 4000 Liège, Belgium
[2] Astrophysique et Spectroscopie, Université de Mons-Hainaut, 7000 Mons, Belgium
[3] Ruhr-Universität Bochum, 44780 Bochum, Germany
[4] Observatoire de Paris[b], 92195 Meudon, France

Received 2 October 2001 / Received in final form 22 January 2002
Published online 28 June 2002 –

Abstract. Transitions between the five fine-structure levels in the $3s^2 3p^3$ ground configuration of Fe XII (P-like) are of interest in astrophysics and terrestrial plasma diagnostics. The decay rates give rise to level lifetimes in the millisecond range, which have been measured recently at a heavy-ion storage ring. While most of the $3s^2 3p^2 3d$ levels are short-lived, two of these levels have no E1 decay channels and may also have millisecond lifetimes. We present HFR and MCDF calculations of the E1, M1, E2 and M2 transition rates between the $3s^2 3p^3$, $3s3p^4$ and $3s^2 3p^2 3d$ levels and compare the lifetime results to most recent experimental data as well as to other predictions.

PACS. 31.15.-p Calculations and mathematical techniques in atomic and molecular physics (excluding electron correlation calculations) – 34.10.+x General theories and models of atomic and molecular collisions and interactions (including statistical theories, transition state, stochastic and trajectory models, etc.) – 32.30.Jc Visible and ultraviolet spectra

1 Introduction

The temperatures in the solar corona are higher than those in the underlying photosphere by several orders of magnitude. This has been found out by identifying various prominent coronal lines in the visible spectrum with transitions among fine-structure levels in highly charged ions, notably of Fe [1]. Some twenty years later, sounding rockets and satellites began to extend the observations of the solar spectrum into the vacuum and extreme ultraviolet (VUV, EUV) spectral ranges. Nowadays spacecrafts like *SOHO* continually monitor EUV emissions of the sun. While the most prominent visible coronal lines of Fe are from Cl-like (Fe X) and Al-like (Fe XIV) ions, the overall charge state distribution favours the spectra Fe X and Fe XI [2]. These and the adjacent spectra of iron feature electric dipole transitions (E1), spin-forbidden E1 *intercombination* transitions, and a multitude of electric-dipole *forbidden* M1, E2 and M2 transitions. Given the not so different level spacings in the $3s^2 3p^k$ ground configurations and the low-lying $3s3p^{k+1}$ and $3s^2 3p^{k-1} 3d$ excited configurations, the various transitions appear in all ranges from the EUV to the infrared (IR).

In all of these ranges, forbidden coronal lines are of astrophysical [3–7] as well as of terrestrial plasma diagnostical interest [8]. A systematic modelling effort that would tie information from all spectral ranges together would be best if complete and correct. However, the experimental level data [9–11] are incomplete by far. Although good spectral observations cover much of the range of interest, a regular finding is that about half of the observed lines remain unidentified [12–14]. Suitable "complete" and accurate calculations are needed to help closing the large gaps. Considering transition probabilities, the situation is even worse. Only for a small fraction of the many levels in highly charged Fe ions that decay by E1 transitions there are experimental level lifetime data, practically all from beam-foil spectroscopy [15–17]. Many of these data are of a precision not better than, say, 10%, because of the limited spectral resolution affordable in the EUV beam-foil spectroscopy of Fe ions, and spectral blends are then a serious impediment. However, the recent development of the heavy-ion storage ring technique for the precise measurement of millisecond-lifetimes [18,19] provides benchmark data on certain types of transitions.

We have elected to perform multi-configuration Dirac-Fock (MCDF) calculations on Fe XII, the P-like spectrum of iron, for various reasons. The spectrum is close to the maximum of the charge state distribution in the solar corona, so the spectral features play a significant role

[a] e-mail: traebert@ep3.ruhr-uni-bochum.de
[b] UMR 8631 (associée au CNRS et à l'université Paris-VII) et DAEC

there [20]. Although several calculations of the level structure of the $3s^23p^3$, $3s3p^4$ and $3s^23p^23d$ configurations exist [3,21,22], none includes the decays of all of these levels. Flower [3] gives lifetime values for the ground configuration levels and branching ratios for electric dipole transitions from the higher-lying levels. While both Huang [21] and Fritzsche *et al.* [22] give level values for all levels in these configurations, Huang presents E1 transition rates for all transitions to the ground configuration, but M1 and E2 rates only within the ground complex. Fritzsche *et al.* [22] present E1 transitions only; a "complete" calculation of a P-like spectrum by this group has been done for low-charge members of the isoelectronic sequence [23]. Numerous other calculations treat the E1-forbidden transitions in the ground configuration only. Thus none of the available calculations covers the decay probabilities of all levels up to the $3d$ levels, and the decay properties of the two $3s^23p^23d$ $J = 9/2$ levels apparently have not been covered at all.

The lifetimes of the four excited levels of the $3s^23p^3$ ground configuration have very recently been measured with notable precision at the heavy-ion storage ring [24]. In the course of that work, the question of a previously untreated, presumably long-lived $3s^23p^23d$ $J = 9/2$ level came up that possibly decays to a notable fraction by M2 transitions, and that might contaminate the decay curves recorded in that experiment. Moreover, we expect that our study will help to identify this level (and others) in solar corona or electron beam ion trap spectra.

2 Calculations

2.1 HFR calculations

The energy level values of the ground configuration of Fe XII (*i.e.* $3s^23p^3$) have been derived from coronal observations [25–29] and carry an uncertainty of ± 5 cm^{-1}. The levels of the $3s3p^4$ and $3s^23p^23d$ configurations, based on observations by Fawcett [30] and by Bromage *et al.* [31] and on refined wavelength measurements by Behring *et al.* [32], feature an uncertainty of ± 10 cm^{-1}. The levels of the $3s^23p^24s$ and $4d$ configurations were derived from wavelength observations by Fawcett *et al.* [33] and show a larger uncertainty of about 200 cm^{-1}. The NIST databases [9,34,35] list 48 levels belonging to the $3s^23p^3$, $3s3p^4$, $3s^23p^23d$, $3s^23p^24s$ and $3s^23p^24d$ configurations. 84 transitions are also given in the spectral range between 6.5805 and 640.6 nm. The energy levels of these compilations were retained for the fitting procedure that is part of the present calculation (see hereafter).

A first computational procedure that we have used for deriving the oscillator strengths and radiative lifetimes in Fe XII is the pseudo-relativistic Hartree-Fock (HFR) method [36]. The calculation performed in the present work was combined with a well-established semi-empirical adjustment of the radial parameters minimizing the differences between computed and experimental energy levels. As we were interested only in lifetimes for levels in the ground and the first excited configurations, the sets of interacting configurations were limited to those with $n = 3$ and $n = 4$ outer electrons. For the odd parity level system, the configurations considered were $3s^23p^3$, $3s^23p3d^2$, $3s3p^33d$, $3p^3d^2$, $3p3d^4$, $3p^5$, $3s^23p^24p$, $3s^23p4p^2$, $3p^44p$, $3s3p^34s$, $3s^23p4s^2$, $3s3p^34d$, $3s^23p4d^2$, $3s^23p^24f$, $3s^23p4f^2$, $3p^44f$, $3s^23p4s4d$, $3s3p^24s4p$, $3s3p^24p4d$ and $3s^23p4p4f$. In the fitting procedure, we have retained all the experimental level values of the odd-parity levels of the ground configuration $3s^23p^3$ (this configuration is the only one that is known experimentally). The adopted parameters were $E_{\rm av} = 74\,658$ cm^{-1}, $F^2(3p,3d) = 131\,642$ cm^{-1}, α (Tree's parameter, see [36], p. 479) $= -79$ cm^{-1} and $\zeta_{3p} = 11\,729$ cm^{-1}. The Slater integrals and the configuration interaction parameters, not adjusted in the fitting procedure, were scaled down to 90% of their *ab initio* values. This procedure simulates the influence of weak interactions with the many configurations that have not been introduced explicitly in the model.

For the even-parity levels, the configurations included in the calculation were $3s3p^4$, $3s^23p^23d$, $3s3p^23d^2$, $3s^23d^3$, $3p^23d^3$, $3s3d^4$, $3p^43d$, $3s^23p^24s$, $3s3p^24s^2$, $3p^44s$, $3s^23p^24d$, $3s3p^24d^2$, $3p^44d$, $3s3p^34p$, $3s3p^24p^2$, $3s3p^34f$, $3s^23p4s4p$, $3s^23p4s4f$, $3s^23p4p4d$ and $3s^23p4d4f$. All the experimentally determined level values were included in the fitting procedure, with the exception of the level at 1 551 400 cm^{-1} ($3s^23p^2(^1{\rm D})\ 4d\ ^2{\rm F}_{5/2}$) which is noted with a question mark in the NIST tables. The same scaling factor (90%) as for the odd-parity configurations was adopted for the parameters of the even-parity configurations.

The adopted parameters (in cm^{-1}) for the low-lying even configurations are given in Table 1. The effective interaction parameter, α, for the $3s^23p^24s$ configuration is considerably larger than the corresponding values of the same parameter for the other configurations of the same table, while the integral $F^2(3p,3p)$ appears somewhat lower than the corresponding values for $3s3p^4$, $3s^23p^23d$ and $3s^23p^24d$ configurations. It should be emphasized however that fixing $\alpha = 0$ for the $3s^23p^24s$ configuration would lead to the following numerical values for the parameters describing this configuration: $E_{\rm av} = 1\,281\,044$ cm^{-1}, $F^2(3p,3p) = 118\,351$ cm^{-1}, $\zeta_{3p} = 11\,526$ cm^{-1}, and $G^1(3p,4s) = 11\,754$ cm^{-1}. It was verified that the effect of this change on the level values or on the transition probabilities and lifetimes values involving the $n = 3$ even parity levels reported in the present paper is entirely negligible. The known levels of the higher-lying configurations were then used as a fit target to adjust the levels produced by our HFR calculations. A level scheme is shown in Figure 1. The calculated HFR level values are compared in Table 2 with the available experimental data. Clearly, the agreement is excellent. It is expected that the predicted values for the experimentally unknown levels are characterized by the same accuracy.

The levels in the ground configuration are metastable, *i.e.*, they cannot decay by emission of electric dipole (E1) radiation. They can decay only through E1-forbidden M1 and E2 transitions. The HFR transition probabilities of all possible transitions within the $3s^23p^3$ configuration can be found in Table 3. They agree quite well with the

Table 1. HFR parameters (in cm^{-1}) adopted for the low lying even configurations of Fe XII; ratio = fitted value/*ab initio* value.

configuration	parameter	value	ratio	configuration	parameter	value	ratio
$3s3p^4$	E_{av}	394 941		$3s^23p^24s$	E_{av}	1 280 046	
	$F^2(3p,3p)$	136 243	0.970		$F^2(3p,3p)$	98 724	0.692
	α	−235			α	1 228	
	ζ_{3p}	11 828	1.057		ζ_{3p}	11 037	0.950
	$G^1(3s,3p)$	169 736	0.925		$G^1(3p,4s)$	11 706	0.714
$3s^23p^23d$	E_{av}	518 500		$3s^23p^24d$	E_{av}	1 548 019	
	$F^2(3p,3p)$	135 735	0.966		$F^2(3p,3p)$	137 921	0.966
	α	−178			α	−480	
	ζ_{3p}	12 123	1.083		ζ_{3p}	11 592	0.999
	ζ_{3d}	583	0.574		ζ_{4d}	356	1.000
	$F^2(3p,3d)$	125 740	0.904		$F^2(3p,4d)$	37 737	0.772
	$G^1(3p,3d)$	148 154	0.922		$G^1(3p,4d)$	10 915	0.925
	$G^3(3p,3d)$	92 739	0.893		$G^3(3p,4d)$	11 803	0.927

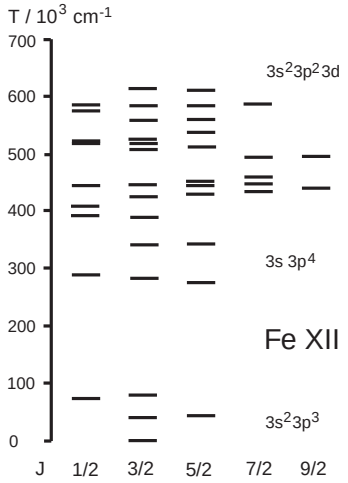

Fig. 1. Level scheme of Fe XII.

MCDF results (see below). The corresponding lifetime values are reported in Table 4 where they are compared with recent very accurate experimental data obtained by Träbert *et al.* [24]. More precisely, the agreement theory-experiment is within about 7%.

A further test of the accuracy of the HFR calculation results from a comparison of the lifetime values derived for the $3s3p^4$ and $3s^23p^23d$ levels with the MCDF data recently obtained by Fritzsche *et al.* [22] for the E1 transitions (the role played by the forbidden lines being negligible as far as the lifetime values are concerned). The comparison is illustrated in Table 5. The agreement (for the length form, which is the only one considered in Cowan's code) is within 10% for the $3s3p^4$ levels and within 20% for the $3s^23p^23d$ levels, with the exception of the (^{1}D) $3d$ $^2F_{5/2,7/2}$ levels where larger discrepancies are observed. In fact, for these two levels, both sets of theoretical data are unreliable: on the one hand, large discrepancies between Coulomb and Babushkin gauge results, in the MCDF approximation, indicate inaccurate wavefunctions; on the other hand, severe cancellation effects are affecting the HFR transition probabilities of some of the lines depopulating the levels of interest. The cancellation factor, CF, as defined by Cowan [36] (p. 432), is given by

$$CF = \left[\frac{|\sum\sum C_{\alpha J}\left\langle \alpha J||P^{(1)}||\alpha' J'\right\rangle C_{\alpha' J'}|}{\sum\sum |C_{\alpha J}\left\langle \alpha J||P^{(1)}||\alpha' J'\right\rangle C_{\alpha' J'}|}\right]^2 \quad (1)$$

if the wavefunctions, for each parity, are expanded in terms of a suitable set of basis functions $|\alpha J\rangle$, $C_{\alpha J}$ representing the mixing coefficients, and $P^{(1)}$ the dipole moment of the atom. Small values of CF (typically < 0.05) indicate large cancellation effects.

2.2 MCDF calculations

The MCDF method was also considered in the present work in order to extend the Fritzsche *et al.* [22] set of results to forbidden M1, E2 and M2 transitions and also to derive new data for the two $J = 9/2$ metastable levels not considered by Fritzsche *et al.* [22] in their paper. The atomic state functions (ASF) of the lowest Fe XII levels were approximated using the GRASP92 package [37] that implements the multiconfigurationnal Dirac-Fock method, MCDF [38]. It consists in representing the ASF as a superposition of configuration state functions (CSF) according to:

$$\Psi(\alpha \Pi J M) = \sum c_i(\alpha)\Phi(\beta_i \Pi J M) \quad (2)$$

where Ψ and Φ are the ASF and the CSF respectively. Π, J and M are the relevant quantum numbers, *i.e.*, the parity, the total angular momentum and its associated total magnetic number, respectively. α and β stand for all the other quantum numbers that are necessary to describe unambiguously the ASF and the CSF. The summation in (1) is extended to n_c the number of CSF in the expansion. Each CSF is built from antisymmetrized products of relativistic

Table 2. Experimental and theoretical energy levels of Fe XII.

level	energy (cm^{-1})			
	experiment	theory (this work)		theory
		HFR	MCDF(\$)	(previous)[c]
$3s^2 3p^3\ {}^4S^o_{3/2}$	0[a]	0	0	0
$^2D^o_{3/2}$	41 555[b]	41 518	42 140	42 667
$^2D^o_{5/2}$	46 088[b]	46 122	46 910	47 130
$^2P^o_{1/2}$	74 108[b]	74 142	75 050	75 532
$^2P^o_{3/2}$	80 515[a]	80 484	81 657	81 792
$3s3p^4\ {}^4P_{5/2}$	274 373[a]	274 234	274 558	274 620
$^4P_{3/2}$	284 005[a]	283 996	-	284 131
$^4P_{1/2}$	288 307[a]	288 429	-	288 431
$^2D_{3/2}$	339 761[b]	339 937	-	341076
$^2D_{5/2}$	341 703[a]	341 797	343 318	342 949
$^2P_{3/2}$ (*1)	389 706[a]	389 277	-	391 660
$^2P_{1/2}$ (*2)	394 120[a]	394 517	-	396 725
$^2S_{1/2}$	-	411 216	-	412 875
$3s^2 3p^2(^3P)3d\ {}^4F_{3/2}$	-	426 384	-	427 998
$^4F_{5/2}$	-	429 957	431 893	432 138
$^4F_{7/2}$	-	435 393	437 688	437 629
$^4F_{9/2}$	-	442 252	444 123	-
$^4D_{1/2}$	-	446 124	-	448 620
$^4D_{7/2}$	-	446 513	448 679	448 714
$^4D_{3/2}$	-	447 173	-	449 684
$^4D_{5/2}$	-	451 720	454 138	454 327
$^2P_{3/2}$ (*3)	501 800[a]	501 758	-	507 969
$^2P_{1/2}$ (*4)	513 850[a]	513 923	-	519 685
$^4P_{5/2}$	513 708[b]	512 278	517 687	517 607
$^4P_{3/2}$	516 740[a]	516 941	-	521 616
$^4P_{1/2}$	519 770[a]	520 102	-	524 750
$^2F_{5/2}$	576 740[a]	576 274	584 166	583 339
$^2F_{7/2}$	581 180[a]	580 907	588 655	587 646
$^2D_{5/2}$	603 930[a]	603 898	611 581	610 608
$^2D_{3/2}$	605 480[a]	605 875	-	612 019
$3s^2 3p^2(^1D)3d\ {}^2F_{5/2}$	-	442 823	444 484	444 461
$^2F_{7/2}$ (*5)	-	461 570	463 474	463 593
$^2G_{7/2}$	-	495 024	497 465	496 836
$^2G_{9/2}$	-	497 170	500 267	-
$^2D_{3/2}$	554 030[a]	554 224	-	559 669
$^2D_{5/2}$	554 610[a]	554 573	560 526	559 753
$^2P_{1/2}$	568 940[a]	569 721	-	575 735
$^2P_{3/2}$	577 740[a]	578 103	-	583 519
$^2S_{1/2}$	579 630[a]	578 754	-	585 712
$3s^2 3p^2(^1S)3d\ {}^2D_{3/2}$	526 120[a]	526 280	-	529 723
$^2D_{5/2}$ (*6)	538 040[a]	537 534	541 965	541 101

[a] NIST [9,34,35], [b] [11], [c] [22], (\$) MCDF-A for the $3s^2 3p^3$ levels. MCDF-B for the others, * strongly mixed levels with the following LS coupling compositions (in %): (1) 44.6 (^{3}P)$3d$ ^{2}P + 45.7 $3s3p^4$ ^{2}P, (2) 30.8 (^{3}P)$3d$ ^{2}P + 34.9 $3s3p^4$ ^{2}P + 23.8 $3s3p^4$ ^{2}S, (3) 42.8 $3s3p^4$ ^{2}P + 24.9 (^{3}P)$3d$ ^{2}P + 24.4 (^{1}D)$3d$ ^{2}P, (4) 37.6 $3s3p^4$ ^{2}P + 29.2 (^{1}D)$3d$ ^{2}P + 21.4 (^{3}D)$3d$ ^{2}P, (5) 30.2 (^{1}D)$3d$ ^{2}F + 42.0 (^{3}P)$3d$ ^{4}D + 21.2 (^{3}P)$3d$ ^{2}F, (6) 40.0 (^{1}S)$3d$ ^{2}D + 41.2 (^{3}P)$3d$ ^{2}D.

Table 3. Calculated (HFR and MCDF-A) transition probabilities for M1 and E2 transitions within the ground configuration $3s^2 3p^3$ of Fe XII.

transition		$A_{ki}(\mathrm{s}^{-1})$	
		HFR	MCDF*
$^4\mathrm{S}^\mathrm{o}_{3/2}$–$^2\mathrm{D}^\mathrm{o}_{3/2}$	M1	5.41(1)	5.52(1)
	E2	4.30(−2)	
$^4\mathrm{S}^\mathrm{o}_{3/2}$–$^2\mathrm{D}^\mathrm{o}_{5/2}$	M1	2.13(0)	2.12(0)
	E2	1.07(−1)	1.06(−1)/1.06(−1)
$^4\mathrm{S}^\mathrm{o}_{3/2}$–$^2\mathrm{P}^\mathrm{o}_{1/2}$	M1	1.90(2)	1.92(2)
	E2	1.23(−1)	1.55(1)/9.95(−2)
$^4\mathrm{S}^\mathrm{o}_{3/2}$–$^2\mathrm{P}^\mathrm{o}_{3/2}$	M1	3.45(2)	3.46(2)
	E2	1.07(−2)	
$^2\mathrm{D}^\mathrm{o}_{3/2}$–$^2\mathrm{D}^\mathrm{o}_{5/2}$	M1	9.28(−1)	8.70(−1)
	E2	4.60(−6)	
$^2\mathrm{D}^\mathrm{o}_{3/2}$–$^2\mathrm{P}^\mathrm{o}_{1/2}$	M1	7.07(1)	7.08(1)
	E2	8.32(−1)	1.92(−1)/7.85(−1)
$^2\mathrm{D}^\mathrm{o}_{3/2}$–$^2\mathrm{P}^\mathrm{o}_{3/2}$	M1	1.99(2)	2.00(2)
	E2	6.40(−1)	6.23(−1)/6.11(−1)
$^2\mathrm{D}^\mathrm{o}_{5/2}$–$^2\mathrm{P}^\mathrm{o}_{3/2}$	M1	7.92(1)	8.05(1)
	E2	1.22(0)	1.21/1.18
$^2\mathrm{D}^\mathrm{o}_{5/2}$–$^2\mathrm{P}^\mathrm{o}_{1/2}$	M1	-	-
	E2	2.93(−1)	1.68(−4)/2.68(−1)
$^2\mathrm{P}^\mathrm{o}_{1/2}$–$^2\mathrm{P}^\mathrm{o}_{3/2}$	M1	1.98(0)	2.03
	E2	1.46(−5)	

* Babushkin/Coulomb gauge results for E2 transitions. For the MCDF results, only the values $A > 0.1$ s^{-1} are given.

spin-orbitals. In the expansion (1), in the framework of the active space method, the list of CSF of a given symmetry is generated by excitations from one or more reference configurations to an active set of orbitals. The coefficients, c_i, together with the orbitals are optimized by minimizing an energy functional. The latter is built from one or more eigenvalues of the Dirac-Coulomb Hamiltonian depending upon the optimization option adopted. Transverse Breit interaction as well as other QED interactions, like vacuum polarization and self-energy, have been added to the Hamiltonian matrix as perturbations.

In the present work, two MCDF calculations were performed (hereafter designated as MCDF-A and MCDF-B).

MCDF-A was dedicated to the determination of lifetime values of all four excited states ($^2\mathrm{D}^\mathrm{o}_{3/2,5/2}$, $^2\mathrm{P}^\mathrm{o}_{1/2,3/2}$) of the ground configuration. For that purpose, all the M1 and E2 transitions between the five states $3s^2 3p^3$ $J = 1/2$, 3/2, 5/2 were considered. The calculations were done in five steps. In the first step, we included only the 5 CSF hereabove mentioned and performed an average level (AL) optimization of the $n = 1, 2$ core orbitals together with the $3s$ and $3p$ orbitals. The second step consisted in considering up to quadruple virtual excitations within the $n = 3$ shell generating a list of 386 CSF. The $3l$ orbitals were optimized by minimising an energy functional built on the five levels of the ground configuration using the extended optimal level (EOL) option of GRASP code. The core orbitals were kept fixed. In the following steps, single and double excitations into $n = 4$, $n = 5$ and $n = 6$ shells were added step by step to the above mentioned CSF list. During each step, the newly introduced orbitals were optimized fixing the others and minimising the same energy functional as during the preceding step. The lists generated in that way contained 2 365, 7 917 and 18 613 CSF, respectively.

MCDF-B was focussed on the radiative decay properties of the two $J = 9/2$ energy levels belonging to the $3s^2 3p^2 3d$ configuration. The 21 CSF of the $3s^2 3p^3$ $J = 3/2$, 5/2, $3s3p^4$ $J = 5/2$ and $3s^2 3p^2 3d$ $J = 5/2$, 7/2, 9/2 configurations were considered in order to calculate all the possible E2, M1 and M2 branches of interest. The ground configuration ($3s^2 3p^3$ $J = 3/2$) was considered to position the levels with respect to its energy. The MCDF-B calculations were performed in three steps. In the first one, up to quadruple excitations within the $n = 3$ shell were included using the 21 above mentioned CSF as reference configurations. It led to a total of 665 CSF. The $n = 1$–3 orbitals were optimized minimizing a functional built from the 21 lowest levels within the EOL option. Single and double virtual excitations into the $n = 4$ shell were then added in the second step leading to a total of 10 164 CSF. Only the $4l$ orbitals were varied using the same energy functional as in the first step. In the final step, only single excitations into the $5l$ subshells were included leading to a total of 11 062 CSF. In fact, computer limitations prevented the inclusion of further correlations, *i.e.* the double excitations into the $n = 5$ shell. As in the preceding step, only the $5l$ orbitals were optimized fixing the others within the same EOL framework.

3 Results and discussion

Table 2 shows a comparison of our calculated energies of the 21 levels belonging to the reference configurations with published experimental values. In Table 4, the radiative lifetimes of the $3s^2 3p^3$ $^2\mathrm{D}^\mathrm{o}_{3/2,5/2}$ energy levels are reported. The MCDF lifetime of the $3s^2 3p^3$ $^2\mathrm{D}^\mathrm{o}_{3/2}$ level agrees quite well with the HFR result and with the recent measurement by Träbert *et al.* [24]. The MCDF lifetime value of the $J = 5/2$ level within the same term is slightly higher than the experiment, whereas the HFR result agrees with the experimental finding within the latter's uncertainty. The presently calculated data are in better agreement with the experimental data from the heavy-ion storage ring [24] than with the data obtained by using an electrostatic ion trap [45]. This may well reflect the smaller systematic errors encountered in the former technique [48]. Similar calculations for P-like Kr^{21+} ions have recently been found to agree with experimental lifetime data from an electron beam ion trap [49], so that now there is a demonstration of reliability along a fair section of the isoelectronic sequence.

The estimates of the $3s^2 3p^2$ (^{3}P) $3d$ $^4\mathrm{F}_{9/2}$ and $3s^2 3p^2$ (^{1}D) $3d$ $^2\mathrm{G}_{9/2}$ level lifetimes are also given, in both gauges, in the fourth column of Table 4. Table 6 lists the major

Table 4. Predicted and observed decays, and measured lifetimes τ (in ms) for metastable levels in Fe XII. Wavelengths are approximate and based on observation, indirect evidence (calculated multiplet structure) or calculation (see text). The MCDF calculational results have been obtained in two gauges (Babushkin/Coulomb), which in the nonrelativistic limit correspond to the length and velocity forms of the transition operator.

upper level	λ(nm)	τ (ms)			
		HFR	MCDF-A	experiment	previous results
$3s^23p^3\ {}^2D^o_{3/2}$	240.6	18.46	18.0/18.0#	20.35 ± 1.24[h]	18.9[a], 18.9[b], 5.0[c], 16.8[d],16.0[e],
				18.0 ± 0.1[i]	20.8[f], 18.4[g], 22.57[h]
$3s^23p^3\ {}^2D^o_{5/2}$	217	315.8	323/323#	306 ± 10[i]	324[a], 115[b], 326[c], 294[d], 313[e],
					544[f], 314[g]
$3s^23p^3\ {}^2P^o_{1/2}$	307.3, 356.7	3.82	3.59/3.79#	4.38 ± 0.42[h]	3.84[a], 3.84[b], 3.84[c], 3.64[d], 3.58[e],
				4.10 ± 0.12[i]	4.05[f], 3.81[g]
$3s^23p^3\ {}^2P^o_{3/2}$	256.7, 290.3	1.59	1.59/1.59#	1.85 ± 0.24[h]	1.61[a], 1.61[b], 2.39[c], 1.55[d], 1.53[e],
				1.70 ± 0.08[i]	1.67[f], 1.59[g]
$3s^23p^2(^3P)3d\ {}^4F_{9/2}$	IR/EUV	- *	11.6/9.2		
$3s^23p^2(^1D)3d\ {}^2G_{9/2}$	195, 275	- *	4.00/4.27		

[a] [39], [b] [40], [c] [41], [d] [42], [e] [21], [f] [43], [g] [44], [h] [45], [i] [24], * some transitions depopulating these levels are affected by cancellation effects in HFR calculations: the corresponding lifetimes could be very inaccurate and, consequently, are not quoted, # corrected for the experimental wavelengths.

Table 5. Comparison of the HFR theoretical lifetimes with those calculated by Fritzsche *et al.* [22] (in s) in the $3s3p^4$ and $3s^23p^23d$ configurations. $a(-b)$ denotes a^{-b}.

		lifetime τ (s)	
level	$E_{\rm exp}$(cm^{-1})[a]	HFR[b]	MCDF [c]
$3s3p^4\ {}^4P_{5/2}$	274 373	5.78(−10)	6.11(−10)/6.17(−10)
$^4P_{3/2}$	284 005	5.38(−10)	5.70(−10)/5.78(−10)
$^4P_{1/2}$	288 307	5.09(−10)	5.40(−10)/5.49(−10)
$^2D_{3/2}$	339 761	2.54(−10)	2.75(−10)/2.78(−10)
$^2D_{5/2}$	341 703	2.81(−10)	3.02(−10)/3.05(−10)
$^2P_{3/2}$	389 706	1.00(−10)	1.10(−10)/1.08(−10)
$^2P_{1/2}$	394 120	8.99(−11)	9.75(−11)/9.48(−11)
$^2S_{1/2}$	411 216*	1.11(−10)	1.18(−10)/1.14(−10)
$3s^23p^2\ (^3P)\ 3d\ {}^4F_{3/2}$	426 384*	4.83(−9)	5.27(−9)/4.97(−9)
$^4F_{5/2}$	429 957*	7.79(−9)	9.32(−9)/8.84(−9)
$^4F_{7/2}$	435 393*	3.61(−8)	3.88(−8)/3.72(−8)
$^4D_{1/2}$	446 124*	1.43(−9)	1.55(−9)/1.48(−9)
$^4D_{7/2}$	446 513*	3.08(−8)	2.89(−8)/2.41(−8)
$^4D_{3/2}$	447 173*	1.40(−9)	1.56(−9)/1.49(−9)
$^4D_{5/2}$	451 720*	1.99(−9)	2.29(−9)/2.20(−9)
$^2P_{3/2}$	501 800	1.40(−11)	1.40(−11)/1.34(−11)
$^2P_{1/2}$	513 850	1.39(−11)	1.38(−11)/1.32(−11)
$^4P_{5/2}$	513 708	1.11(−11)	1.11(−11)/1.08(−11)
$^4P_{3/2}$	516 740	1.10(−11)	1.12(−11)/1.06(−11)
$^4P_{1/2}$	519 770	1.05(−11)	1.05(−11)/1.01(−11)
$^2F_{5/2}$	576 740	9.10(−12)	9.12(−12)/8.95(−12)
$^2F_{7/2}$	581 180	9.11(−12)	9.13(−12)/8.96(−12)
$^2D_{5/2}$	603 930	1.01(−11)	1.02(−11)/9.98(−12)
$^2D_{3/2}$	605 480	1.04(−11)	1.03(−11)/9.88(−12)
$3s^23p^2\ (^1D)\ 3d\ {}^2F_{5/2}$	442 823*	6.93(−9)§	1.02(−8)/9.77(−9)
$^2F_{7/2}$	461 570*	4.77(−7)§	1.36(−5)/7.28(−5)
$^2G_{7/2}$	495 024*	3.32(−9)	3.92(−9)/3.77(−9)
$^2D_{3/2}$	554 030	1.27(−11)	1.27(−11)/1.22(−11)
$^2D_{5/2}$	554 610	1.96(−11)	1.78(−11)/1.74(−11)
$^2P_{1/2}$	568 940	1.41(−11)	1.36(−11)/1.30(−11)
$^2P_{3/2}$	577 740	1.35(−11)	1.33(−11)/1.26(−11)
$^2S_{1/2}$	579 630	1.37(−11)	1.36(−11)/1.32(−11)
$3s^23p^2\ (^1S)\ 3d\ {}^2D_{3/2}$	526 120	5.54(−11)	5.31(−11)/5.03(−11)
$^2D_{5/2}$	538 040	2.83(−11)	3.29(−11)/3.15(−11)

[a] From NIST compilations [34,35]. Values marked with an asterisk (*) are theoretical HFR estimates. [b] HFR: this work (length form). [c] Fritzsche *et al.* [22] (L/V: length form/velocity form). § Affected by cancellation effects.

Table 6. Transition probabilities A for the most intense lines ($A > 0.1$ s^{-1}) depopulating the $3s^2 3p^2$ (^{3}P) $3d$ ^{4}F$_{9/2}$ and $3s^2 3p^2$ (^{1}D) $3d$ ^{2}G$_{9/2}$ energy levels.

Transition		Type	λ/(nm)	A (s^{-1})	
			calculated	MCDF*	HFR
$3s^2 3p^2(^3\mathrm{P})3d\ ^4\mathrm{F}_{9/2}$	$-\ 3s3p^4\ ^2\mathrm{D}_{5/2}$	E2	99.2	0.126/0.237	0.065
	$-\ 3s3p^4\ ^4\mathrm{P}_{5/2}$	E2	59.0	40.3/62.5	0.319§
	$-\ 3s^2 3p^2 3d\ ^4\mathrm{F}_{7/2}$	M1	1 484.8	7.75	8.03
	$-\ 3s^2 3p^3\ ^2\mathrm{D}^{\mathrm{o}}_{5/2}$	M2	25.2	38.2	- [a]
$3s^2 3p^2(^1\mathrm{D})3d\ ^2\mathrm{G}_{9/2}$	$-\ 3s^2 3p^2(^3\mathrm{P})3d\ ^4\mathrm{F}_{7/2}$	E2	193.8	0.232/0.245	0.002
	$-\ 3s^2 3p^2(^3\mathrm{P})3d\ ^4\mathrm{F}_{9/2}$	E2	178.1	0.268/0.280	8.82(−6)§
	$-\ 3s^2 3p^2(^1\mathrm{D})3d\ ^2\mathrm{F}_{5/2}$	E2	146.3	0.665/0.075	-
	$-\ 3s3p^4\ ^2\mathrm{D}_{5/2}$	E2	63.7	45.5/19.9	20.18
	$-\ 3s3p^4\ ^4\mathrm{P}_{5/2}$	E2	44.3	0.387/10.6	1.48
	$-\ 3s^2 3p^2(^1\mathrm{D})3d\ ^2\mathrm{G}_{7/2}$	M1	3 567.6	0.259	0.117
	$-\ 3s^2 3p^2(^3\mathrm{P})3d\ ^4\mathrm{D}_{7/2}$	M1	271.8	8.38	8.89
	$-\ 3s^2 3p^2(^3\mathrm{P})3d\ ^4\mathrm{F}_{7/2}$	M1	193.8	4.75	7.10
	$-\ 3s^2 3p^2(^3\mathrm{P})3d\ ^4\mathrm{F}_{9/2}$	M1	178.1	120	127.6
	$-\ 3s^2 3p^2(^1\mathrm{D})3d\ ^2\mathrm{F}_{7/2}$	M1	159.0	63.3	36.7
	$-\ 3s^2 3p^3\ ^3\mathrm{D}^{\mathrm{o}}_{5/2}$	M2	22.1	6.08	- [a]

* MCDF (third step; see text); Babushkin/Coulomb for E2 transitions, [a] M2 rates are not available from Cowan's HFR code, § strong cancellation effects in the HFR calculation.

decay branches of these two levels. It should be emphasized that the M2 contributions play a significant role here because they contribute by about 44% and 2%, respectively, to the total decay rates. However, the HFR transition probabilities (no M2) of some transitions depopulating the two levels of interest are affected by cancellation effects in the line strengths and induce, consequently, large uncertainties in the HFR lifetime values.

Obviously, experimental data that would test the lifetime calculations for these two levels would be particularly welcome, as they would also inform on details of the atomic structure and wave functions. However, the decay branches of the (^{3}P) $3d$ ^{4}F$_{9/2}$ level are in the infrared (M1 decay to the $J = 7/2$ level of the same term) and in the EUV (E2 and M2 decays to the $J = 5/2$ levels of the $3s^2 3p^3$ and $3s3p^4$ configurations). Neither spectral range is covered in the recent work at any ion trap, especially the heavy-ion storage ring [24]. The IR decay branch may be of interest in the wide field of applications of IR coronal lines [7].

The situation is better for the (^{1}D) $3d$ ^{2}G$_{9/2}$ level, as our calculations indicate decay branches in the UV and near vacuum-UV (Tab. 6), a range suitable for the experimental set-up at the heavy-ion storage ring. Considering both HFR and MCDF calculations, we expect the strongest decay branches near 178–182 nm and the next (and already much) weaker ones near 272–281 nm and near 194 nm. Our calculations are not precise enough to pinpoint the wavelengths of these decay branches to better than some ±3%. This, in fact, leaves open whether one or both of the decay branches are just inside or just outside the detection range of the solar-blind detector (with a long-wavelength cut-off near 280 nm) that was used in the heavy-ion storage ring experiment (outside a sapphire window of the vacuum vessel), and whether at the short-wavelength end the transmission of air near a wavelength of 180 nm was sufficiently high.

However, even without any spectrally resolved observation of the decays there is an indication that the emission from the (^{1}D) $3d$ ^{2}G$_{9/2}$ level did play a role. Our calculated lifetime values agree rather well with three of the four precisely measured lifetimes of ground-configuration levels. The shortest-lived, however, has been reported at (1.70±0.02) ms compared to our prediction of near 1.6 ms. Considering the experimental conditions and a common decay curve with (assumedly) three components, we see it as quite likely (from our calculations) that the 1.7 ms fit component represents a superposition of one major decay component of 1.6 ms and a weaker one of 4 ms. While extracting such a fourth decay component from a fit to the data may be overextending fit procedures and statistics, we take it as an implicit confirmation of our predictions. A direct measurement, using narrow-band filters, should in principle be possible. It would clearly be helped if the emission lines could first be identified in solar spectra or the emission spectrum of an electron beam ion trap, so that the actual wavelengths became available. We expect that our present calculations narrowed down the range of search.

This work was financially supported by the a cultural agreement between the French CNRS and the Belgian FNRS-CGRI. EB and CJZ are indebted to the Observatoire de Paris and the IPNAS for excellent hospitality. EB is Research Director of

the Belgian FNRS. ET gratefully acknowledges support by a Belgian FNRS research grant and the cordial hospitality experienced at the IPNAS.

References

1. B. Edlén, Z. Astrophysik **22**, 30 (1942)
2. H.E. Mason, H. Nussbaumer, Astron. Astrophys. **54**, 547 (1977)
3. D.R. Flower, Astron. Astrophys. **54**, 163 (1977)
4. M. Kafatos, J.P. Lynch, Astrophys. J. Suppl. Ser. **42**, 611 (1980)
5. M. Eidelsberg, F. Crifo-Magnant, C.J. Zeippen, Astron. Astrophys. Suppl. Ser. **43**, 455 (1981)
6. J.P. Lynch, M. Kafatos, Astrophys. J. Suppl. Ser. **76**, 1169 (1991)
7. M.A. Greenhouse, U. Feldman, H.A. Smith, M. Klapisch, A.K. Bhatia, A. Bar-Shalom, Astrophys. J. Suppl. Ser. **88**, 23 (1993)
8. B. Edlén, Phys. Scripta T **8**, 5 (1984)
9. J. Sugar, C. Corliss, J. Phys. Chem. Ref. Data Suppl. **14**, 2 (1985)
10. K. Mori, M. Otsuka, T. Kato, *Grotrian Diagrams of Highly Ionized Iron, Fe VIII-Fe XVI* (Institute of Plasma Physics, Nagoya University, 1977)
11. C. Jupén, R.C. Isler, E. Träbert, Mon. Not. R. Astron. Soc. **264**, 627 (1993)
12. G.D. Sandlin, G.E. Brueckner, R. Tousey, Astrophys. J. **214**, 898 (1977)
13. G.D. Sandlin, J.-D.F. Bartoe, G.E. Brueckner, R. Tousey, M.E. van Hoosier, Astrophys. J. Suppl. Ser. **61**, 801 (1986)
14. U. Feldman, W.E. Behring, W. Curdt, U. Schühle, K. Wilhelm, P. Lemaire, T.M. Moran, Astrophys. J. Suppl. Ser. **113**, 195 (1997)
15. R. Hutton, Nucl. Instrum. Meth. B **31**, 294 (1988)
16. E. Träbert, P.H. Heckmann, R. Hutton, I. Martinson, J. Opt. Soc. Am. B **5**, 2173 (1988)
17. E. Träbert, Mon. Not. R. Astron. Soc. **297**, 399 (1998)
18. J. Doerfert, E. Träbert, A. Wolf, D. Schwalm, O. Uwira, Phys. Rev. Lett. **78**, 4355 (1997)
19. E. Träbert, A. Wolf, J. Linkemann, X. Tordoir, J. Phys. B **32**, 537 (1999)
20. F.P. Keenan, R.J. Thomas, W.M. Neupert, V.J. Foster, P.J.F. Brown, S.S. Tayal, Mon. Not. R. Astron. Soc. **278**, 773 (1996)
21. K.-N. Huang, At. Data Nucl. Data Tables **30**, 313 (1984)
22. S. Fritzsche, C. Froese Fischer, B. Fricke, At. Data Nucl. Data Tables **68**, 149 (1998)
23. S. Fritzsche, B. Fricke, D. Geschke, A. Heitmann, J.E. Sienkiewicz, Astrophys. J. **518**, 994 (1999)
24. E. Träbert, G. Gwinner, A. Wolf, E.J. Knystautas, H.-P. Garnir, X. Tordoir, J. Phys. B: At. Mol. Opt. Phys. **35**, 671 (2002)
25. W.M. Burton, A. Ridgeley, R. Wilson, Mon. Not. R. Astron. Soc. **135**, 207 (1967)
26. G.A. Doschek, U. Feldman, M.E. van Hoosier, J.-D.F. Bartoe, Astrophys. J. Suppl. Ser. **31**, 417 (1976)
27. A.H. Gabriel, W.R.S. Garton, L. Golberg, T.J.L. Jones, C. Jordan, F.J. Morgan, R.W. Nicholls, W.J. Parkinson, H.J.B. Paxton, E.M. Reeves, C.B. Shenton, R.J. Speer, R. Wilson, Astrophys. J. **169**, 595 (1971)
28. J.T. Jefferies, Mem. Soc. Roy. Sci. Liège **17**, 213 (1969)
29. L.A. Svensson, Solar Phys. **18**, 232 (1971)
30. B.C. Fawcett, J. Phys. B **4**, 1577 (1971)
31. G.E. Bromage, R.D. Cowan, B.C. Fawcett, Astrophys. J. **203**, 521 (1978)
32. W.E. Behring, L. Cohen, U. Feldman, G.A. Doschek, Astrophys. J. **203**, 52 (1976)
33. B.C. Fawcett, R.D. Cowan, E.Y. Kononov, R.W. Hayes, J. Phys. B **5**, 1255 (1972)
34. J.R. Fuhr, G.A. Martin, W.L. Wiese, J. Phys. Chem. Ref. Data **17**, Suppl. 4, 493 (1988)
35. J.R. Fuhr, W.C. Martin, A. Musgrove, J. Sugar, W.L. Wiese, NIST Atomic Spectroscopic Database, at `http://physics.nist.gov/PhysRefData/contents.html`
36. R.D. Cowan, *The Theory of Atomic Structures and Spectra* (University of California Press, Berkeley CA, 1981)
37. F.A. Parpia, C. Froese Fischer, I.P. Grant, Comput. Phys. Commun. **94**, 249 (1996)
38. I.P. Grant, Meth. Comp. Chem. **2**, 1 (1988)
39. R.H. Garstang, Opt. Pura Apl. **5**, 192 (1972)
40. M.W. Smith, W.L. Wiese, J. Phys. Chem. Ref. Data **2**, 85 (1973)
41. R. Smitt, L.Å. Svensson, M. Outred, Phys. Scripta **13**, 293 (1976)
42. C. Mendoza, C.J. Zeippen, Mon. Not. R. Astron. Soc. **198**, 127 (1982)
43. V. Kaufman, J. Sugar, J. Phys. Chem. Ref. Data **15**, 321 (1986)
44. E. Biémont, J.E. Hansen, Phys. Scripta **31**, 509 (1985)
45. D.P. Moehs, M.I. Bhatti, D.A. Church, Phys. Rev. A **63**, 032515 (2001)
46. S. Fritzsche, F. Koike, J.E. Sienkiewicz, N. Vaeck, Phys. Scripta T **80**, 479 (1999)
47. S. Fritzsche, C.Z. Dong, E. Träbert, Mon. Not. R. Astron. Soc. **318**, 263 (2000)
48. E. Träbert, Phys. Scripta T **92**, 444 (2001)
49. E. Träbert, P. Beiersdorfer, G.V. Brown, H. Chen, D.B. Thorn, E. Biémont, Phys. Rev. A **64**, 042411 (2001)